Proceedings of the European Control Conference 2007
Kos, Greece, July 2-5, 2007

Three Dimensional Trajectory Control of Underactuated AUVs

Filoktimon Repoulias and Evangelos Papadopoulos

Abstract— **This paper considers the design of a novel closed-loop trajectory tracking controller for an underactuated AUV having 6 degrees of freedom (DOF) and 3 controls, namely a thruster, a rudder and moving surfaces to control the forward, yaw and pitch motions respectively. A backstepping methodology is adopted as a design tool since it is suitable for the cascaded nature of the vehicle dynamics. It also offers flexibility and robustness against parametric uncertainties which are often encountered in hydrodynamic modeling. Indeed, in our simulations we assume a 10% error in hydrodynamic parameters and yet the controller performs the task of position, orientation and linear and angular velocity tracking successfully.**

Index Terms— **Trajectory Tracking Control, Underactuated AUV.**

I. Introduction

AUTONOMOUS Underwater Vehicles (AUVs), such as the one shown in Fig. 1, have been playing a major role in exploration and exploitation of resources located in deep oceanic environments. They are employed in risky missions such as oceanic observations, bathymetric surveys, ocean floor analysis, military applications, etc., [1]. Apart from their numerous practical applications, these vehicles present a challenging control problem since most of them are underactuated, i.e., they have fewer inputs than DOF. Such control configurations impose non-integrable acceleration constraints. Furthermore, AUVs' kinematic and dynamic models are highly non-linear and coupled making control design a difficult task, [2]. Underactuation rules out the use of customary control schemes e.g. full state-feedback linearization, [3], and the strong hydrodynamic effects exclude designs based solely on the kinematic model. When moving on a horizontal plane, AUVs present similar dynamic behavior to underactuated surface vessels, [2].

The stabilization problem, i.e. regulation to a point for surface vessels and AUVs has been studied in [4]-[6]. It is shown that such vehicles cannot be asymptotically stabilized by continuous time-invariant feedback control laws.

During many missions, AUVs undertake the task of tracking an inertial trajectory (a space curve with a specified

Manuscript received October 16, 2006.

F. Repoulias is with the Dept. of Mech. Eng., National Technical University of Athens (NTUA), Greece (e-mail: firepoul@central.ntua.gr).

E. Papadopoulos is with the Dept. of Mech. Eng., National Technical University of Athens (NTUA), Greece (corresponding author, phone: +(30) 210-772-1440; fax: +(30) 210-772-1455; e-mail: egpapado@central.ntua.gr).

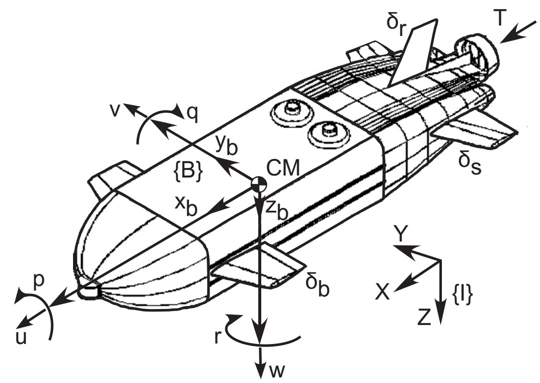

Fig. 1. The AUV with the body-fixed frame, the controls and motion variables.

timing law). This requires the design of control laws that guide and keep the vehicle on the trajectory regardless of external disturbances, modeling errors etc.

Tracking controller designs for underactuated marine vehicles currently in use follow classical approaches such as local linearization and decoupling of the multivariable model aiming at steering as many degrees of freedom as the available control inputs. This is done using linearization about trimming trajectories (trajectories with constant velocities) that lead to time invariant linear systems followed by such techniques as gain scheduling, [7]. In the same work, the authors design a parameterized family of linear controllers about trimming trajectories. They require accurate knowledge of the hydrodynamic model, while stability results at the switching points between different controllers and tracking performance of the velocity errors are not provided. The validity of these solutions is limited in a small neighborhood around the selected operating points. Stability and performance also suffer significantly when the vehicle executes maneuvers that amplify the action of its complex hydrodynamics and nonlinear coupling terms.

Theoretical and experimental results on trajectory tracking for underactuated marine vehicles show that nonlinear Lyapunov-based techniques can overcome most of the limitations mentioned above. The authors in [8], present experimental tracking results for a model ship using Lyapunov-based controllers. In [9], two tracking solutions for a surface vessel were proposed, based on Lyapunov's direct method and passivity approach. However, in the last three works, the yaw velocity was required to be nonzero. Under this restriction, straight lines cannot be tracked. In [10], the error dynamics is transformed into a skew-symmetric form and practical convergence is achieved. The

ISBN: 978-960-89028-5-5

authors in [11] have designed a controller for vehicles moving in two or three dimensions that exponentially forces the position tracking error to a small neighborhood of the origin. However, the attitude of the vehicle is left uncontrolled, which may lead to trajectory tracking but with a wrong heading. In addition, the stability of the velocities was not investigated. In [12], the combined problem of trajectory planning and tracking control for an underactuated AUV moving on the horizontal plane was studied. The controller design was based on backstepping techniques and the position and orientation errors as well as linear and angular velocity errors asymptotically converged to zero. This is the first work in the control literature in which trajectory planning, based on the dynamic model, for underactuated marine vehicles was presented. In [13], the same planning and tracking control methodology was applied in the case of a nontrimming trajectory with time-varying velocities — a sinusoidal path — where also parametric inaccuracies were considered. The results of trajectory planning were extended in [14] for underactuated AUVs moving in 3D, also a new result. The importance of trajectory planning lies in the consistency of the generated desired variables — position, orientation and linear and angular velocities — with vehicle dynamics. Incorporating these variables in a closed-loop tracking controller alleviates its efforts and leaves for the latter the task of error convergence and compensation of parametric inaccuracies only.

In this paper, we present a novel closed-loop tracking controller for an underactuated AUV moving in 3D space and having 3 controls, namely a thruster to control surge motion, and a rudder and lateral moving surfaces to control yaw and pitch motion respectively. We adopt the backstepping design methodology, as this suits the cascaded nature of the vehicle dynamics, and gains from the inherent robustness of Lyapunov techniques. To demonstrate the efficiency of this controller we present simulations in which we assume errors in the hydrodynamic parameters of the order of 10%. The results show that the controller is successful in all cases.

II. AUV Kinematics and Dynamics

A. Kinematics

In this section, the kinematic and dynamic equations of motion for an AUV moving in a 3D space are presented.

To describe the kinematics, two reference frames are employed, the inertial reference frame $\{I\}$ and a body-fixed frame $\{B\}$, see Fig. 1. As shown, the origin of the $\{B\}$ frame coincides with the AUV center of mass (CM) while the center of buoyancy (CB) is on the negative z body axis for static stability. Using the standard notation of ocean engineering, the general motion of an AUV in 6 DOF can be described by the following vectors:

$$\begin{aligned}&\boldsymbol{\eta}=[\boldsymbol{\eta}_1^T,\boldsymbol{\eta}_2^T]^T;\quad \boldsymbol{\eta}_1=[x,y,z]^T;\quad \boldsymbol{\eta}_2=[\phi,\theta,\psi]^T;\\ &\mathbf{v}=[\mathbf{v}_1^T,\mathbf{v}_2^T]^T;\quad \mathbf{v}_1=[u,\upsilon,w]^T;\quad \mathbf{v}_2=[p,q,r]^T;\end{aligned}\tag{1}$$

In (1), $\boldsymbol{\eta}_1$ denotes the inertial position of the CM and $\boldsymbol{\eta}_2$ the orientation of $\{B\}$ with respect to (wrt) the $\{I\}$ frame in terms of Euler angles. Vector $\mathbf{v}_1$ denotes the linear velocity of the CM and $\mathbf{v}_2$ the angular velocity of $\{B\}$ wrt the $\{I\}$ frame, both expressed in the body-fixed $\{B\}$ frame.

In guidance and control applications, for the representation of rotations, it is customary to use the xyz (roll-pitch-yaw) convention defined in terms of Euler angles, adopted in the present work, or quaternions. In this work, we use the first approach. Hence, the velocity transformation between the $\{B\}$ and the $\{I\}$ frames is expressed as

$$\dot{\boldsymbol{\eta}}_1=\mathbf{J}_1(\boldsymbol{\eta}_2)\mathbf{v}_1\tag{2}$$

where

$$\mathbf{J}_1(\boldsymbol{\eta}_2)=\begin{bmatrix}c\psi c\theta & -s\psi c\phi+c\psi s\theta s\phi & s\psi s\phi+c\psi c\phi s\theta\\ s\psi c\theta & c\psi c\phi+s\phi s\theta s\psi & -c\psi s\phi+s\theta s\psi c\phi\\ -s\theta & c\theta s\phi & c\theta c\phi\end{bmatrix}\tag{3}$$

The body-fixed angular velocitiy, and the time rate of the Euler angles are related through

$$\dot{\boldsymbol{\eta}}_2=\mathbf{J}_2(\boldsymbol{\eta}_2)\mathbf{v}_2\tag{4}$$

where

$$\mathbf{J}_2(\boldsymbol{\eta}_2)=\begin{bmatrix}1 & s\phi t\theta & c\phi t\theta\\ 0 & c\phi & -s\phi\\ 0 & s\phi/c\theta & c\phi/c\theta\end{bmatrix}\tag{5}$$

where $s\cdot=\sin(\cdot)$, $c\cdot=\cos(\cdot)$, $t\cdot=\tan(\cdot)$.

B. Dynamics

The dynamic model of the AUV presented in [2] is employed here. It is a simplified model developed for control design tasks, and captures the main dynamical characteristics of a flat-fish shaped AUV moving in 3D space, see Fig. 1. The vehicle is underactuated, i.e., it has less control inputs than the number of DOF. Specifically, in the following equations of motion, the three controls are surge propulsion T, rudder angle δ_r for yaw rotation, and stern and bow plane angles $\delta_s=-\delta_b$ for pitch rotation. The equations of motion are,

$$\begin{aligned}(m-r_3X_{\dot u})\dot u&=(r_3X_{wq}-m)wq+(r_3X_{vr}+m)\upsilon r\\&\quad+r_2X_{uu}u^2+r_2X_{vv}\upsilon^2+T\end{aligned}\tag{6a}$$

$$(m-r_3Y_{\dot v})\dot\upsilon=(r_3Y_r-m)ur+(r_3Y_{wp}+m)wp+r_2Y_vu\upsilon\tag{6b}$$

$$(m-r_3Z_{\dot w})\dot w=(r_3Z_q+m)uq+(r_3Z_{vp}-m)\upsilon p+r_2Z_wuw\tag{6c}$$

$$(I_x-r_5K_{\dot p})\dot p=r_5K_{qr}qr+r_4K_pup+z_{CB}c\theta s\phi B\tag{6d}$$

$$\begin{aligned}(I_y-r_5M_{\dot q})\dot q&=(r_5M_{pr}+I_z-I_x)pr+r_4M_{uq}uq+r_3M_{uw}uw\\&\quad+r_3u^2(M_{ds}\delta_s+2M_{db}\delta_b)+z_{CB}s\theta B\end{aligned}\tag{6e}$$

$$(I_z - r_5 N_{\dot r})\dot r = (r_5 N_{qp} + I_x - I_y) pq + r_3 N_v u\upsilon \\ + r_4 N_r ur + r_3 u^2 N_{dr}\delta_r \tag{6f}$$

A brief explanation of the various terms and the values of the main ones in (6) follows: $m = 5454.54$ kg is the vehicle's mass, and $I_x = 2038\ \mathrm{Nms}^2$, $I_y = 13587\ \mathrm{Nms}^2$, and $I_z = 13587\ \mathrm{Nms}^2$ are the moments of inertia about the body x_b, y_b, and z_b, axes respectively. The term B is the buoyancy force acting on the CB. The term z_{CB} is the $z-$coordinate of the CB.,

$$r_i = (\rho/2)L^i \qquad i = 1,...,5 \tag{7}$$

where ρ is the water density and $L = 5.3$ m the AUVs length. $X_{\dot u}$, $Y_{\dot v}$, $Z_{\dot w}$ are added mass terms and $K_{\dot p}$, $M_{\dot q}$, $N_{\dot r}$ are added moments of inertia terms. X_{wq}, X_{vr}, Y_r, Y_{wp}, Z_q, Z_{vp}, K_{qr}, M_{pr}, and N_{qp} are added mass cross terms. X_{uu}, X_{vv}, Y_v, Z_w, K_p, M_{uq}, M_{uw}, M_{ds}, M_{db}, N_v, N_r, and N_{dr} are drag and body lift, force and moment terms. Detailed description and the values of the model parameters can be found in [2]. The lack of control actuation in sway υ, heave w, and roll p motions renders the system underactuated.

III. Trajectory Tracking Control Design

In this section, the trajectory tracking control design is presented. We assume bounded reference velocities and nonzero surge velocity.

A. Reference Variables

The reference 6 DOF trajectory to be tracked by the AUV is generated by a trajectory planning algorithm developed in [14]. In this subsection, we briefly describe this planning methodology.

Let a smooth 3D trajectory to be followed by the CM of the AUV be given by its inertial coordinates x_R, y_R, and z_R. From now on, the subscript "R" denotes a reference (desired) variable. Associating the Frenet frame to every point of the curve, we can also derive the "orientation" of the trajectory. This orientation is not the reference one since the body-fixed frame, as the CM tracks the reference path, undergoes a further rotation wrt the Frenet frame due to the dynamics. This rotation is described by the angles of attack and sideslip which are functions of the body-fixed linear velocities. Hence, we also derive the reference Euler angles ϕ_R, θ_R, and ψ_R. The reference angular velocities p_R, q_R, and r_R are then obtained by differentiation and the fact that the angular velocity of the body frame wrt the inertial frame is the sum of the angular velocity of the body frame wrt the Frenet frame and the angular velocity of the Frenet frame wrt the inertial frame. The linear, body-fixed velocities u_R, υ_R, and w_R are obtained considering the equality of the total AUV velocity and the trajectory velocity, and the integration of the two unactuated dynamic equations (6b) and (6c).

We conclude that this planning methodology provides the full, 6 DOF trajectory, consistent with AUV's dynamics. Using this feasible trajectory, the design of closed-loop tracking controllers can be facilitated and result in improved performance since the controller has only to deal with the tracking error convergence and compensation of parametric inaccuracies.

B. Error Dynamics Formulation

Using the states of the vehicle and the reference variables, the tracking errors are defined as

$$\begin{aligned} &u_e = u - u_R,\ \upsilon_e = \upsilon - \upsilon_R,\ w_e = w - w_R, \\ &p_e = p - p_R,\ q_e = q - q_R,\ r_e = r - r_R, \\ &x_e = x - x_R,\ y_e = y - y_R,\ z_e = z - z_R, \\ &\phi_e = \phi - \phi_R,\ \theta_e = \theta - \theta_R,\ \psi_e = \psi - \psi_R \end{aligned} \tag{8}$$

From (2) and (4) it is

$$\dot{\boldsymbol{\eta}}_{1R} = \mathbf{J}_1(\boldsymbol{\eta}_{2R})\mathbf{v}_{1R} \tag{9a}$$

$$\dot{\boldsymbol{\eta}}_{2R} = \mathbf{J}_2(\boldsymbol{\eta}_{2R})\mathbf{v}_{2R} \tag{9b}$$

Then, the kinematics tracking errors are written as

$$\dot{\boldsymbol{\eta}}_{1e} = \mathbf{J}_1(\boldsymbol{\eta}_2)\mathbf{v}_1 - \mathbf{J}_1(\boldsymbol{\eta}_{2R})\mathbf{v}_{1R} \tag{10a}$$

$$\dot{\boldsymbol{\eta}}_{2e} = \mathbf{J}_2(\boldsymbol{\eta}_2)\mathbf{v}_2 - \mathbf{J}_2(\boldsymbol{\eta}_{2R})\mathbf{v}_{2R} \tag{10b}$$

Substituting in these $\mathbf{v}_1 = \mathbf{v}_{1e} + \mathbf{v}_{1R}$, $\mathbf{v}_2 = \mathbf{v}_{2e} + \mathbf{v}_{2R}$, yields

$$\dot{\boldsymbol{\eta}}_{1e} = \mathbf{J}_1(\boldsymbol{\eta}_2)\mathbf{v}_{1e} + \boldsymbol{\mu}_1 \tag{11a}$$

$$\dot{\boldsymbol{\eta}}_{2e} = \mathbf{J}_2(\boldsymbol{\eta}_2)\mathbf{v}_{2e} + \boldsymbol{\mu}_2 \tag{11b}$$

where

$$\boldsymbol{\mu}_1 = [\mathbf{J}_1(\boldsymbol{\eta}_2) - \mathbf{J}_1(\boldsymbol{\eta}_{2R})]\mathbf{v}_{1R} \tag{12a}$$

$$\boldsymbol{\mu}_2 = [\mathbf{J}_2(\boldsymbol{\eta}_2) - \mathbf{J}_2(\boldsymbol{\eta}_{2R})]\mathbf{v}_{2R} \tag{12b}$$

are both treated as bounded (for bounded reference velocities) time-varying disturbances.

Considering the dynamics, assuming $u \neq 0$ (which is natural for tracking purposes), and setting

$$T = -[(r_3 X_{wq} - m)wq + (r_3 X_{vr} + m)\upsilon r + \\ r_2 X_{uu} u^2 + r_2 X_{vv}\upsilon^2] + (m - r_3 X_{\dot u})\tau_u \tag{13}$$

$$\delta_s = [1/r_3 u^2 (M_{ds} - 2M_{db})][[(I_x - r_5 M_{pr} - I_z)pr - \\ r_4 M_{uq} uq - r_3 M_{uw} uw - z_{CB} s\theta B] + (I_y - r_5 M_{\dot q})\tau_q] \tag{14}$$

$$\delta_r = (1/r_3 u^2 N_{dr})[[(I_y - r_5 N_{qp} - I_x)pq - r_3 N_v u\upsilon \\ - r_4 N_r ur] + (I_z - r_5 N_{\dot r})\tau_r] \tag{15}$$

we obtain the following partially linearized system:

$$\dot u_e = -\dot u_R + \tau_u \tag{16a}$$

$$\dot\upsilon_e = [(r_3 Y_r - m)/(m - r_3 Y_{\dot\upsilon})]ur_e + \varepsilon_\upsilon \tag{16b}$$

$$\dot w_e = [(r_3 Z_q + m)/(m - r_3 Z_{\dot w})]uq_e + \varepsilon_w \tag{16c}$$

$$\dot{p}_e = [(r_4K_p)/(I_x - r_5K_{\dot{p}})]u_e p_e + \varepsilon_{p1} \tag{16d}$$

$$\dot{q}_e = -\dot{q}_R + \tau_q \tag{16e}$$

$$\dot{r}_e = -\dot{r}_R + \tau_r \tag{16f}$$

where τ_u, τ_q, and τ_r are auxiliary controls and the ε terms are given by,

$$\begin{aligned}\varepsilon_\upsilon = -\dot{\upsilon}_R + [(r_3Y_r - m)(u_e r_R + u_R r_R) + \\ (r_3Y_{wp} + m)(w_e + w_R)(p_e + p_R) + \\ r_2Y_v(u_e + u_R)(\upsilon_e + \upsilon_R)]/(m - r_3Y_{\dot{\upsilon}})\end{aligned} \tag{17a}$$

$$\begin{aligned}\varepsilon_w = -\dot{w}_R + [(r_3Z_q + m)(u_e q_R + u_R q_R) + \\ (r_3Z_{vp} - m)(\upsilon_e + \upsilon_R)(p_e + p_R) + \\ r_2Z_w(u_e + u_R)(w_e + w_R)]/(m - r_3Z_{\dot{w}})\end{aligned} \tag{17b}$$

$$\begin{aligned}\varepsilon_{p1} = -\dot{p}_R + [r_5K_{qr}(q_e + q_R)(r_e + r_R) + \\ r_4K_p(up_R + p_e u_R) + \\ z_{CB}c(\theta_e + \theta_R)s(\phi_e + \phi_R)B]/(I_x - r_5K_{\dot{p}})\end{aligned} \tag{17c}$$

C. Error Dynamics Stabilization

In the sequel, we proceed to the design of a control law for the underactuated system of (11a) and (11b), and (16a)-(16f) using the backstepping and nonlinear damping methodology

Before proceeding to the design steps, we make a few observations: Firstly, considering (16), we note that the directly controlled variables are the velocities u_e, q_e, and r_e, using τ_u, τ_q, and τ_r respectively. Secondly, in order to control the positioning (11a) and orientation (11b) subsystems we shall use in a first step, as virtual controls, the velocities u_e, υ_e, w_e, and p_e, q_e, r_e, respectively. But υ_e, w_e, and p_e, are not directly controlled; yet, we can exploit the coupling terms $(r_3Y_r - m)ur$, $(r_3Z_q + m)uq$, and $r_4K_p up$ in the dynamic equations, and the nonzero surge velocity assumption to control these variables.

.***Step 1***. Considering the subsystem (11b), we take as virtual controls the vector $\mathbf{v}_{2e} = [p_e, q_e, r_e]^T$ and for now we ignore the term $\boldsymbol{\mu}_2$. Then, the first part of the desired expressions for the virtual controls is chosen as

$$\mathbf{v}_{2e,des} = -\mathbf{J}_2^{-1}(\mathbf{K}_2 + \mathbf{K}_3)\boldsymbol{\eta}_{2e} \triangleq \boldsymbol{\alpha}_{\mathbf{v}2} = [\alpha_p, \alpha_{q1}, \alpha_{r1}]^T \tag{18}$$

where $\mathbf{K}_2 \triangleq diag(k_2, k_2, k_2)$ and $\mathbf{K}_3 \triangleq diag(k_3, k_3, k_3)$ are positive definite gain matrices. The inversion of $\mathbf{J}_2$ results in the singular point $\theta = \pm\pi/2$; this is not a problem if the vehicle is not going to operate near this point. The component α_p is the desired value for the velocity p_e, but since this is not a real control, we introduce the error variable $z_p = p_e - \alpha_p$. Then, from (16d) it is

$$\dot{z}_p = [(r_4K_p)/(I_x - r_5K_{\dot{p}})]u_e p_e + \varepsilon_p \tag{19a}$$

where

$$\varepsilon_p = \varepsilon_{p1} - \dot{\alpha}_p \tag{19b}$$

to be treated in a later step. Also, the variables α_{q1} and α_{r1} are the parts of $q_{e,des}$ and $r_{e,des}$ respectively used to control the rotational kinematics. Selecting u_e as a virtual control in (19a), and since the term $[(r_4K_p)/(I_x - r_5K_{\dot{p}})]$ is negative, our choice is

$$u_{e,pdes} = \tanh(p_e)c_p z_p \triangleq \alpha_{u,p} \tag{20}$$

which is the part of $u_{e,des}$ that controls z_p. In (20), we used the hyperbolic tangent function because it is smooth and it compromises the signs as needed. Considering the subsystem (11a), we take as virtual controls the vector $\mathbf{v}_{1e} = [u_e, \upsilon_e, w_e]^T$ and set

$$\mathbf{v}_{1e,des} = -\mathbf{J}_1^T(\mathbf{K} + \mathbf{K}_1)\boldsymbol{\eta}_{1e} \triangleq \boldsymbol{\alpha}_1 = [\alpha_{u,\eta1}, \alpha_\upsilon, \alpha_w]^T \tag{21}$$

where $\mathbf{K} \triangleq diag(k, k, k)$ and $\mathbf{K}_1 \triangleq diag(k_1, k_1, k_1)$ are positive definite gain matrices. The component $\alpha_{u,\eta1} \triangleq u_{e,\eta des}$ is the part of the velocity $u_{e,des}$ that controls inertial velocities and

$$\alpha_u = \alpha_{u,p} + \alpha_{u,\eta1} \tag{22}$$

Returning to (11a), and (19a), and the controls (20) and (22), we note that the components of the vector $\boldsymbol{\alpha}_{\mathbf{v}1} \triangleq [\alpha_u, \alpha_\upsilon, \alpha_w]^T$ are not true controls. Hence, we introduce appropriate error variables:

$$\mathbf{z}_u = [z_u, z_\upsilon, z_w]^T \triangleq [u_e - \alpha_u, \upsilon_e - \alpha_\upsilon, w_e - \alpha_w]^T \tag{23}$$

Then, the controlled subsystem so far is:

$$\dot{\boldsymbol{\eta}}_{1e} = \mathbf{J}_1[\boldsymbol{\alpha}_{\mathbf{v}1} + \mathbf{z}_u] + \boldsymbol{\mu}_1 \tag{24}$$

$$\dot{z}_p = [(r_4K_p)/(I_x - r_5K_{\dot{p}})]p_e\alpha_{u,p} + f_p \tag{25a}$$

with

$$f_p = f_p(\alpha_{u,\eta1}, \varepsilon_p) \tag{25b}$$

This function will be bounded when the complete system controller is designed at the final step.

The task now is to stabilize the inertial position $\boldsymbol{\eta}_{1e}$ and the error variables z_p and z_u. In this step, z_u is stabilized using τ_u. Choosing

$$V_1 = (\boldsymbol{\eta}_{1e}^T\boldsymbol{\eta}_{1e} + z_p^2 + z_u^2)/2 \tag{26}$$

its time derivative becomes

$$\begin{aligned}\dot{V}_1 = -\boldsymbol{\eta}_{1e}^T(\mathbf{K} + \mathbf{K}_1)\boldsymbol{\eta}_{1e} + \boldsymbol{\eta}_{1e}^T\boldsymbol{\mu}_1 + c_p z_p \tanh(p_e)(x_e c\psi c\theta + \\ y_e c\theta s\psi - z_e s\theta) + z_w[z_e c\phi c\theta + y_e(c\phi s\psi s\theta - c\psi s\phi) + \\ x_e(s\phi s\psi + c\phi c\psi s\theta)] + z_\upsilon[z_e c\theta s\phi + y_e(s\phi s\psi s\theta + \\ c\phi c\psi) + x_e(c\psi s\phi s\theta - c\phi s\psi)] + c_p[(r_4K_p)/(I_x - \\ r_5K_{\dot{p}})]\tanh(p_e)p_e z_p^2 + z_p[(r_4K_p)/(I_x - r_5K_{\dot{p}})]\alpha_{u,\eta1}p_e \\ + z_p f_p + z_u[\tau_u - \dot{u}_R - \dot{\alpha}_u + x_e c\psi c\theta + y_e c\theta s\psi - \\ z_e s\theta + z_p[(r_4K_p)/(I_x - r_5K_{\dot{p}})]p_e]\end{aligned} \tag{27}$$

Using Young's inequality [3], nonlinear damping [15], and setting

$$\tau_u = \dot{u}_R - c_{zu1} z_u - c_{zu3} z_u^3 + \dot{\alpha}_u - x_e c\psi c\theta - y_e c\theta s\psi \\ + z_e s\theta - z_p [(r_4 K_p)/(I_x - r_5 K_{\dot{p}})] p_e] \tag{28}$$

and after some algebraic manipulations, (27) becomes

$$\dot{V}_1 \le -\boldsymbol{\eta}_{1e}^T (\mathbf{K} - \boldsymbol{\Lambda}) \boldsymbol{\eta}_{1e} + [\|\boldsymbol{\mu}_1\|^2 / 4k_1] + \gamma_1 + \\ c_p [(r_4 K_p)/(I_x - r_5 K_{\dot{p}})] \tanh(p_e) p_e z_p^2 + \\ [(z_\upsilon^2 + z_w^2)/4\lambda] - [c_{zu1} - (1/4\lambda)] z_u^2 - c_{zu3} z_u^4 \tag{29a}$$

where $\boldsymbol{\Lambda} \triangleq diag(\lambda, \lambda, \lambda)$ is a positive definite gain matrix, $k > \lambda$, and c_{zu1}, c_{zu3} are positive constants with $c_{zu1} > 1/4\lambda$. Also, γ_1 is a smooth function with undefined sign yet:

$$\gamma_1 = \gamma_1 (z_p, x_e, y_e, z_e, \alpha_{u,\eta 1}, p_e) \tag{29b}$$

Step 2. We now consider the stabilization of the subsystems that are controlled by the assumed virtual controls r_e and q_e, i.e., the rotational kinematics and the errors z_υ and z_w the dynamics of which are written as

$$\dot{z}_\upsilon = [(r_3 Y_r - m)/(m - r_3 Y_{\dot{\upsilon}})] u r_e + \varepsilon_\upsilon - \dot{\alpha}_\upsilon \tag{30}$$

$$\dot{z}_w = [(r_3 Z_q + m)/(m - r_3 Z_{\dot{w}})] u q_e + \varepsilon_w - \dot{\alpha}_w \tag{31}$$

Here, we choose

$$q_{e,wdes} = -c_q [(r_3 Z_q + m)/(m - r_3 Z_{\dot{w}})] u z_w \triangleq \alpha_{q2} \tag{32}$$

$$r_{e,\upsilon des} = -c_r [(r_3 Y_r - m)/(m - r_3 Y_{\dot{\upsilon}})] u z_\upsilon \triangleq \alpha_{r2} \tag{33}$$

where c_q and c_r are positive constants. Then, taking into account (18) it is

$$\alpha_r = \alpha_{r1} + \alpha_{r2} \tag{34}$$

$$\alpha_q = \alpha_{q1} + \alpha_{q2} \tag{35}$$

So far, the controlled subsystem of the rotational kinematics and the errors z_υ and z_w is transformed as

$$\dot{z}_\upsilon = -c_r [(r_3 Y_r - m)/(m - r_3 Y_{\dot{\upsilon}})]^2 u^2 z_\upsilon + f_\upsilon \tag{36}$$

$$\dot{z}_w = -c_q [(r_3 Z_q + m)/(m - r_3 Z_{\dot{w}})]^2 u^2 z_w + f_w \tag{37}$$

$$\dot{\boldsymbol{\eta}}_{2e} = -(\mathbf{K}_2 + \mathbf{K}_3) \boldsymbol{\eta}_{2e} + \boldsymbol{\mu}_2 + \mathbf{f}_{\eta 2} \tag{38}$$

with

$$f_\upsilon = f_\upsilon (\varepsilon_\upsilon, \dot{\alpha}_\upsilon, \theta_e, \psi_e) \tag{39a}$$

$$f_w = f_w (\varepsilon_w, \dot{\alpha}_w, \theta_e, \psi_e) \tag{39b}$$

$$\mathbf{f}_{\eta 2} = \mathbf{f}_{\eta 2} (z_w, z_\upsilon) \tag{39c}$$

In order to stabilize the above subsystem, we choose

$$V_2 = (\boldsymbol{\eta}_{1e}^T \boldsymbol{\eta}_{1e} + \boldsymbol{\eta}_{2e}^T \boldsymbol{\eta}_{2e} + z_p^2 + z_u^2 + z_\upsilon^2 + z_w^2)/2 \tag{40}$$

Taking into account (29a), and using nonlinear damping, its time derivative becomes

$$\dot{V}_2 \le -\boldsymbol{\eta}_{1e}^T (\mathbf{K} - \boldsymbol{\Lambda}) \boldsymbol{\eta}_{1e} - \boldsymbol{\eta}_{2e}^T \mathbf{K}_2 \boldsymbol{\eta}_{2e} + [\|\boldsymbol{\mu}_1\|^2 / 4k_1] \\ + c_p [(r_4 K_p)/(I_x - r_5 K_{\dot{p}})] \tanh(p_e) p_e z_p^2 \\ + [\|\boldsymbol{\mu}_2\|^2 / 4k_3] + \gamma_2 - [c_{zu1} - (1/4\lambda)] z_u^2 - c_{zu3} z_u^4 \tag{41a}$$

where

$$\gamma_2 = \gamma_2 (\gamma_1, f_\upsilon, f_w, \mathbf{f}_{\eta 2}) \tag{41b}$$

and will be discussed later.

Step 3. The variables p_e, q_e and r_e are not true controls. Thus, we introduce the errors $z_p \triangleq p_e - \alpha_p$, $z_q \triangleq q_e - \alpha_q$ and $z_r \triangleq r_e - \alpha_r$ in (36)-(38) yielding:

$$\dot{z}_\upsilon = -c_r [(r_3 Y_r - m)/(m - r_3 Y_{\dot{\upsilon}})]^2 u^2 z_\upsilon \\ + [(r_3 Y_r - m)/(m - r_3 Y_{\dot{\upsilon}})] u z_r + f_\upsilon \tag{42}$$

$$\dot{z}_w = -c_q [(r_3 Z_q + m)/(m - r_3 Z_{\dot{w}})]^2 u^2 z_w \\ + [(r_3 Z_q + m)/(m - r_3 Z_{\dot{w}})] u z_q + f_w \tag{43}$$

$$\dot{\boldsymbol{\eta}}_{2e} = -(\mathbf{K}_2 + \mathbf{K}_3) \boldsymbol{\eta}_{2e} + \mathbf{J}_2 [z_p, z_q, z_r]^T + \boldsymbol{\mu}_2 + \mathbf{f}_{\eta 2} \tag{44}$$

We choose

$$V_3 = (\boldsymbol{\eta}_{1e}^T \boldsymbol{\eta}_{1e} + \boldsymbol{\eta}_{2e}^T \boldsymbol{\eta}_{2e} + z_p^2 + z_u^2 + z_\upsilon^2 + z_w^2 + z_q^2 + z_r^2)/2 \tag{45}$$

and taking its time derivative we have

$$\dot{V}_3 \le -\boldsymbol{\eta}_{1e}^T (\mathbf{K} - \boldsymbol{\Lambda}) \boldsymbol{\eta}_{1e} - \boldsymbol{\eta}_{2e}^T \mathbf{K}_2 \boldsymbol{\eta}_{2e} + [\|\boldsymbol{\mu}_1\|^2 / 4k_1] \\ + c_p [(r_4 K_p)/(I_x - r_5 K_{\dot{p}})] \tanh(p_e) p_e z_p^2 \\ + [\|\boldsymbol{\mu}_2\|^2 / 4k_3] - [c_{zu1} - (1/4\lambda)] z_u^2 - c_{zu3} z_u^4 \\ - c_r [(r_3 Y_r - m)/(m - r_3 Y_{\dot{\upsilon}})]^2 u^2 z_\upsilon^2 \\ - c_q [(r_3 Z_q + m)/(m - r_3 Z_w)]^2 u^2 z_w^2 \\ + z_r [\tau_r - \dot{r}_R - \dot{\alpha}_r + [(r_3 Y_r - m)/(m - r_3 Y_{\dot{\upsilon}})] u z_\upsilon \\ + \psi_e (c\phi / c\theta) - \theta_e s\phi + \phi_e c\phi t\theta] \\ + z_q [\tau_q - \dot{q}_R - \dot{\alpha}_q + [(r_3 Z_q + m)/(m - r_3 Z_w)] u z_w \\ + \theta_e c\phi + \psi_e (s\phi / c\theta) + \phi_e s\phi t\theta] + \gamma_3 \tag{46}$$

where γ_3 is a smooth function of the states. We now set the controls τ_q and τ_r as follows:

$$\tau_q = \dot{q}_R + \dot{\alpha}_q - [(r_3 Z_q + m)/(m - r_3 Z_w)] u z_w - \theta_e c\phi \\ - \psi_e (s\phi / c\theta) - \phi_e s\phi t\theta] - c_{zq1} z_q - c_{zq3} z_q^3 \tag{47}$$

$$\tau_r = \dot{r}_R + \dot{\alpha}_r - [(r_3 Y_r - m)/(m - r_3 Y_{\dot{\upsilon}})] u z_\upsilon \\ - \psi_e (c\phi / c\theta) + \theta_e s\phi - \phi_e c\phi t\theta - c_{zr1} z_r - c_{zr3} z_r^3 \tag{48}$$

where c_{zq1}, c_{zq3}, c_{zr1}, c_{zr3} are positive constants. Then, (46) becomes

$$\dot{V}_3 \le -\boldsymbol{\eta}_{1e}^T (\mathbf{K} - \boldsymbol{\Lambda}) \boldsymbol{\eta}_{1e} - \boldsymbol{\eta}_{2e}^T \mathbf{K}_2 \boldsymbol{\eta}_{2e} + \gamma_3 + [\|\boldsymbol{\mu}_1\|^2 / 4k_1] \\ + [\|\boldsymbol{\mu}_2\|^2 / 4k_3] + c_p [(r_4 K_p)/(I_x - r_5 K_{\dot{p}})] \tanh(p_e) p_e z_p^2 \\ - c_{zq3} z_q^4 - [c_{zu1} - (1/4\lambda)] z_u^2 - c_{zu3} z_u^4 - c_{zr1} z_r^2 - c_{zr3} z_r^4 \\ - c_r [(r_3 Y_r - m)/(m - r_3 Y_{\dot{\upsilon}})]^2 u^2 z_\upsilon^2 \\ - c_q [(r_3 Z_q + m)/(m - r_3 Z_w)]^2 u^2 z_w^2 - c_{zq1} z_q^2 \tag{49}$$

Before proceeding, we make the following assumptions concerning positive terms like $\|\boldsymbol{\mu}_1\|$, and terms with undefined sign, like the terms contained in γ_3.

Assumptions: 1) Each of the time-varying terms (that stem from the reference trajectory variables) has a constant upper bound (for example $0<\|r_R\|\le r_{R,\max}$). This can be set during trajectory planning.
2) The uncontrolled velocity errors have upper bounds, $\|\upsilon_e\|\le\upsilon_{e,\max}$, $\|w_e\|\le w_{e,\max}$, and $\|p_e\|\le p_{e,\max}$, where $\upsilon_{e,\max}$, $w_{e,\max}$, and $p_{e,\max}$ are positive constants. We can think of these bounds as the maximum admissible operating limits ("flight envelope") beyond which a guidance law is needed.
3) The surge velocity has lower and upper bounds, $\|u\|\le u_{\max}$, where $u_{\max}$ is a positive constant, and $u\neq 0$ as already has been stated.

After tedious but straightforward algebraic manipulations of the various terms in (49), and taking into account the above assumptions, we end up with the following form of the derivative of V_3:

$$\begin{aligned}\dot{V}_3 \le & -\boldsymbol{\eta}_{1e}^T\boldsymbol{\Pi}_1\boldsymbol{\eta}_{1e}-\boldsymbol{\eta}_{2e}^T\boldsymbol{\Pi}_2\boldsymbol{\eta}_{2e}-c_1(p_e)z_p^2\\ & -c_2z_u^2-c_3(u)z_\upsilon^2-c_4(u)z_w^2-c_5z_r^2-c_6z_q^2+c_o\end{aligned} \tag{50}$$

where $\boldsymbol{\Pi}_1\triangleq diag(\pi_1,\pi_1,\pi_1)$ and $\boldsymbol{\Pi}_2\triangleq diag(\pi_2,\pi_2,\pi_2)$ are positive definite gain matrices. The gain $c_1(p_e)$ is positive as long as $p_e\neq 0$. The gains $c_3(u)$ and $c_4(u)$ are positive when $u\neq 0$, and c_2, c_5, and c_6 are positive constants. Also, c_o is a positive constant, which can be made very small using an appropriate combination of the values of the various gains. Now, if we define

$$\mathbf{z}\triangleq[\boldsymbol{\eta}_{1e}^T,\boldsymbol{\eta}_{2e}^T,z_u,z_\upsilon,z_w,z_p,z_q,z_r]^T \tag{51}$$

(45) can be written as,

$$2V_3=\|\mathbf{z}\|^2 \tag{52}$$

Taking $\xi=\min\{\pi_1,\pi_2,c_1,c_2,c_3,c_4,c_5,c_6\}$, then

$$\dot{V}_3\le -2\xi V_3+c_o \tag{53}$$

which, by employing the Comparison Lemma [3], yields

$$V_3(t)\le V_3(0)e^{-2\xi t}+(c_o/2\xi) \tag{54}$$

for $t\in[0,t_{final})$. Doing the algebra, we conclude that

$$\|\mathbf{z}(t)\|\le\|\mathbf{z}(0)\|e^{-\xi t}+\sqrt{c_o/\xi},\quad t\in[0,t_{final}) \tag{55}$$

Eq. (55) means that the states of the error dynamics remain in a bounded set around zero, which can be reduced using an appropriate combination of the controller gains. At this result we arrived using (13), (14), and (15), along with (28), (47), and (48).

IV. Simulation Results

A large number of simulation results showed that the above designed controls perform very well in terms of quick convergence of the tracking errors to zero, smooth transient response, low control effort, and robustness, even in the case of large modeling inaccuracies. To illustrate the performance of the designed trajectory tracking controller, typical simulations are presented.

The reference 6 DOF trajectory is described by the following equations: the reference inertial position for the CM of the vehicle is given by the helix,

$$x_R=70\cos(0.02t)\ \text{m} \tag{56a}$$

$$y_R=70\sin(0.02t)\ \text{m} \tag{56b}$$

$$z_R=0.3t\ \text{m} \tag{56c}$$

Then, following the methodology developed in [14], we compute the reference orientation given by the Euler angles

$$\phi_R=-6.71\times10^{-3}\ \text{rad} \tag{56d}$$

$$\theta_R=-0.211\ \text{rad} \tag{56e}$$

$$\psi_R=0.02t\ \text{rad} \tag{56f}$$

and linear and angular body-fixed velocities

$$u_R=1.431\ \text{m/s} \tag{56g}$$

$$\upsilon_R=-0.0448\ \text{m/s} \tag{56h}$$

$$w_R=0.436\times10^{-3}\ \text{m/s} \tag{56i}$$

$$p_R=4.19\times10^{-3}\ \text{rad/s} \tag{56j}$$

$$q_R=-0.131\times10^{-3}\ \text{rad/s} \tag{56k}$$

$$r_R=0.0196\ \text{rad/s} \tag{56l}$$

The initial errors for the simulations are set as $\|x_e\|=0.3$ m, $\|y_e\|=0.3$ m, $\|z_e\|=0.2$ m, $\|\phi_e\|=\|\theta_e\|=\|\psi_e\|=2$ deg, $\|u_e\|=0.1$ m/s, $\|\upsilon_e\|=0.01$ m/s, $\|w_e\|=10^{-3}$ m/s, and $\|p_e\|=\|q_e\|=\|r_e\|=0$ rad/s.

The dynamic model used is that of (6). However, in order to investigate the robustness of the controller we introduced errors of the order of 10% in all of the hydrodynamic parameters used in the control law.

The following simulations were obtained with controller gains chosen as: $k=k_1=c_{zu1}=3$, $k_2=k_3=c_{zq1}=2$, $c_{zu3}=c_{zr1}=c_{zr3}=c_{zq3}=1$, $c_p=c_r=0.05$, and $c_q=0.1$, all in appropriate SI units. We also impose limits on the angles of rotation of the control surfaces to be $\|\delta\|\le 30$ deg.

In Fig. 2, the reference and the resulting trajectory of the CM of the AUV in the inertial $X-Y-Z$ space are displayed. Fig. 3 shows the control force T, and the rotation of the control surfaces δ_s, δ_b, and δ_r needed for tracking. Bow and stern control surfaces converge smoothly to their steady state values after 5 s, see Fig. 3(b,d). In Fig. 3(f), the rudder reaches the limit of rotation before it converges. The errors in linear velocities are depicted in Fig. 4(a, b, c, d, e, and f). After a short period of time they converge smoothly to a very small neighborhood of zero. The error u_e, as is directly controlled, converges faster, in about 10 s, while the errors υ_e and w_e need 20 s. In Fig. 5(a, b, c, d, e, and f), the tracking errors in the angular velocities are shown. They smoothly converge to zero after 20 s. In Fig. 6(a, b, c, d, e, and f), we can see that the inertial position errors converge in about 15 s, in a small neighborhood of zero, of the order of 5 mm, and slowly oscillate within. Finally, in Fig. 7(a, b, c, d, e, and f), we see the errors of the Euler angles to converge smoothly to their steady state value of the order of 0.3 deg, in about 15 s.

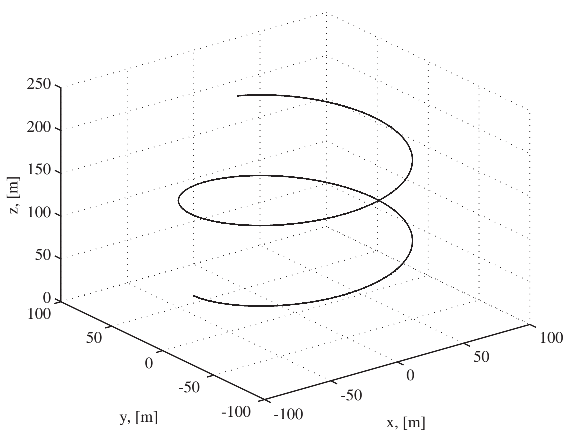

Fig. 2. The actual and the reference 3D space path.

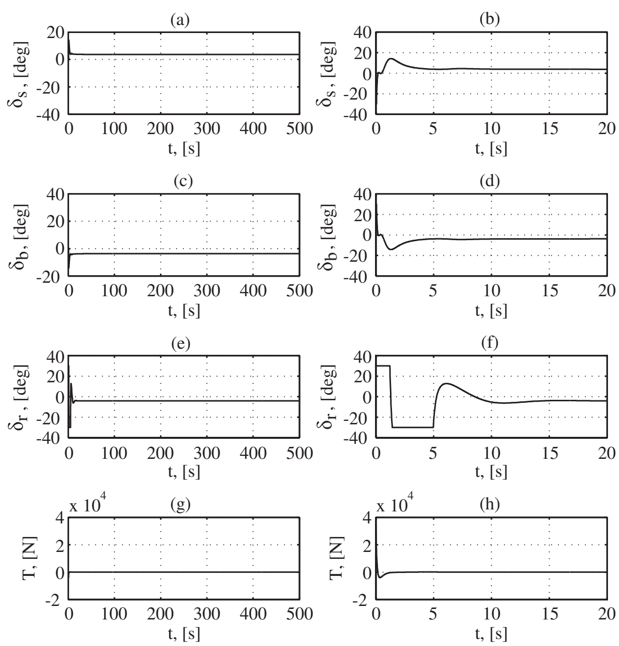

Fig. 3. (a) Stern control surface and, (c) Bow control surface deflections. (e) Rudder deflection. (g) Control force. (b), (d), (f), (h) First 20 s.

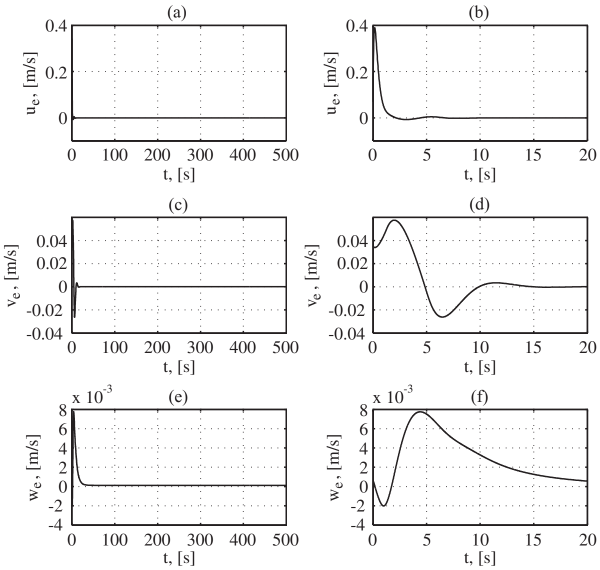

Fig. 4. (a), (c), (e) Linear velocities tracking errors. (b), (d), (f) First 20 s.

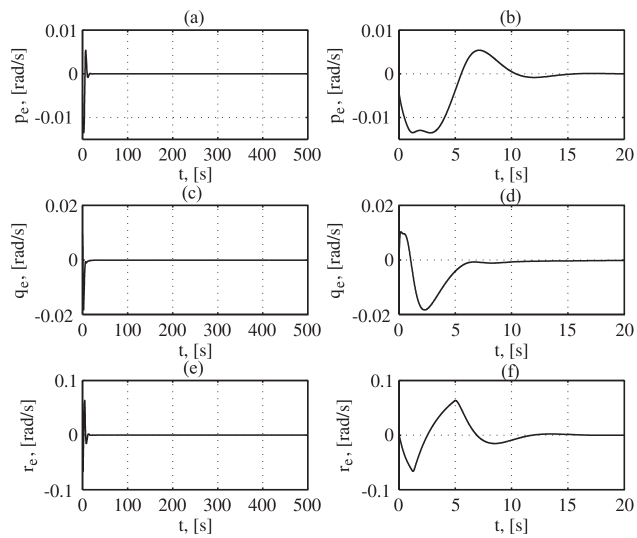

Fig. 5. (a), (c), (e) Angular velocities tracking errors. (b), (d), (f) First 20 s.

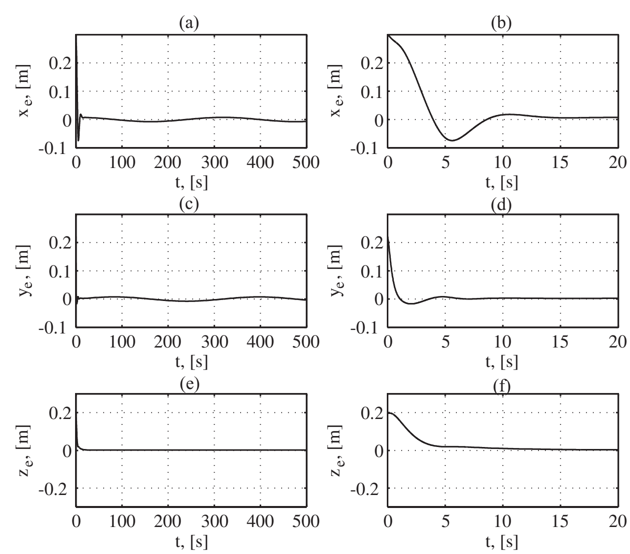

Fig. 6. (a), (c), (e) Inertial positions tracking errors. (b), (d), (f) First 20 s.

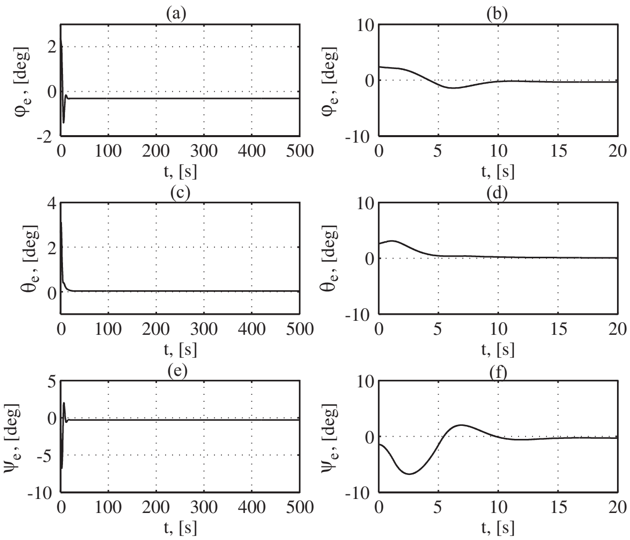

Fig. 7. (a), (c), (e) Euler angles tracking errors. (b), (d), (f) First 20 s.

V. CONCLUSIONS

In this paper, we presented a novel closed-loop tracking controller for an underactuated AUV, in 3D space, having only 3 control inputs. We adopted backstepping as our design methodology, as it offers flexibility and robustness in parametric uncertainties, which is inherent in Lyapunov techniques. To the best of the authors' knowledge, this is a first work in the control literature where successful tracking results are presented in position, orientation and linear and angular velocities, i.e., in full 6 DOF. Moreover, these results were obtained with significant hydrodynamic parameters' errors of 10%, in the structure of the controller which is the case in such environments.

For future work, we intend to present results of the application of the developed tracking controller in the case of trajectories with time-varying velocities. We currently study the derivation of an analytical expression between the gains and the initial tracking errors as well as between the gains and the maximum errors of the unactuated variables. Finally, to avoid Euler angle representational singularities, the representation of kinematics by means of quaternions will be considered.

REFERENCES

[1] J. Yuh, "Design and control of autonomous underwater robots: A survey", *Int. J. Control,* No 8, 2000, pp. 7-24

[2] T. I. Fossen, *Guidance and Control of Ocean Vehicles,* New York: Wiley, 1994.

[3] H. K. Khalil, *Nonlinear Systems,* 2nd ed, Prentice Hall, Upper Saddle River, 1996.

[4] K. Y. Wichlund, O. Sordalen, and O. Egeland, "Control properties of underactuated vehicles", *Proc. IEEE Int. Conf. on Robotics and Automation,* May 1995, pp. 2009-2014.

[5] M. Reyhanoglou, "Exponential stabilization of an underactuated autonomous surface vessel," *Automatica,* 33:12, 1997, pp. 2249-2254.

[6] F. Mazenc, K. Y. Pettersen, and H. Nijmeijer, "Global uniform asymptotic stabilization of an underactuated surface vessel," *IEEE Transactions on Automatic Control,* 47:10, October 2002, pp. 1759-1762.

[7] C. Silvestre, A. Pascoal, and I. Kaminer, "On the design of gain-scheduled trajectory tracking controllers," *Int. J. Robust Nonlinear Control*, 12: 797–839, 2002.

[8] E. Lefeber, K. Y. Pettersen, and H. Nijmeijer, "Tracking control of an underactuated ship," *IEEE Transactions on Control Systems Technology,* Vol. 11, No 1, January 2003, pp. 52-61.

[9] Z. P. Jiang, "Global tracking control of underactuated ships by Lyapunov's Direct Method," *Automatica,* 38:1, 2002, pp.301-309.

[10] A. Behal, D. M. Dawson, W. E. Dixon, and Y. Fang, "Tracking and regulation control of an underactuated surface vessel with nonintegrable dynamics," *IEEE Transactions on Automatic Control,* Vol. 47, No 3, March 2002, pp. 495-500.

[11] P. A. Aguiar, and J. P. Hespanha, "Position tracking of underactuated vehicles", *Pr. ACC,* June 2003.

[12] F. Repoulias, and E. Papadopoulos, "Trajectory planning and tracking control design of underactuated AUVs," *Proc. IEEE Int. Conf. on Robotics and Automation (ICRA 2005),* Barcelona, Spain, 2005, pp.1622-1627.

[13] F. Repoulias, and E. Papadopoulos, "Planar trajectory planning and tracking control design for underactuated AUVs," *Ocean Engineering*, submitted for publication.

[14] F. Repoulias, and E. Papadopoulos, "On spatial trajectory planning & open-loop control for underactuated AUVs," *Proc. 8th IFAC Symposium on Robot Control (SYROCO '06),* Bologna, Italy, September 2006.

[15] M. Krstic, I. Kanellakopoulos, and P. Kokotovic, *Nonlinear and Adaptive Control Design,* New York: Wiley, 1995